Analysis of Histomorphological/molecular Association and Immune Checkpoint Regulators in Epithelioid Glioblastoma and Pleomorphic Xanthoastrocytoma: Are These Tumors Potential Candidate for Immune Checkpoint Blockade

Swati Mahajan
All India Institute of Medical Sciences
Jyotsna Singh
All India Institute of Medical Sciences
Prerna Jha
All India Institute of Medical Sciences
Iman Dandapath
All India Institute of Medical Sciences
Sujata Chaturvedi
IHBAS: Institute of Human Behaviour and Allied Sciences
Arvind Ahuja
Dr Ram Manohar Lohia Hospital PGIMER: Dr Ram Manohar Lohia Hospital and Post Graduate Institute of Medical Education and Research
Minakshi Bhardwaj
Dr Ram Manohar Lohia Hospital PGIMER: Dr Ram Manohar Lohia Hospital and Post Graduate Institute of Medical Education and Research
Ravindra Kumar Saran
Govind Ballabh Pant Institute of Postgraduate Medical Education and Research: Govind Ballabh Pant Hospital
Ajay Garg
All India Institute of Medical Sciences
Mehar Chand Sharma
All India Institute of Medical Sciences
Niveditha Manjunath
All India Institute of Medical Sciences
Ashish Suri
All India Institute of Medical Sciences
Chitra Sarkar

All India Institute of Medical Sciences
Vaishali Suri (surivaishali@yahoo.co.in)
All India Institute of Medical Sciences https://orcid.org/0000-0001-6485-8194

Research Article

Keywords: Epithelioid glioblastoma, Pleomorphic xanthoastrocytoma, BRAF V600E, PDL1, CTLA4, CD3, CD8

Posted Date: March 15th, 2021

DOI: https://doi.org/10.21203/rs.3.rs-296010/v1

Abstract

Introduction

Epithelioid glioblastoma (eGB) was adopted as a provisional entity in the 2016 WHO classification of central nervous tumors. Accurate diagnosis of eGBs and pleomorphic xanthoastrocytoma (PXA) is sometimes challenging owing to overlapping histological and genetic features. There are limited reports on immune profile of these tumors.

Materials and methods

Twenty one PXA's [15 PXA, 6 Anaplastic-PXA (A-PXA) and 14 eGB's were assessed for histopathological and molecular association and their immune profile was compared to primary (1°) GBs (n-18).

Results

PXA cases showed extensive whereas variable positivity for epithelial and glial markers was seen in A-PXAs and eGBs. All cases showed retained nuclear ATRX and INI-1. H3K27M or IDH mutation was seen in none. P53 mutation was more common in eGB's (57%) and A-PXA (33.33%) as compared to PXA (13.33%). None of the 1° GB's harbored *BRAF* V600E, which was observed in 57% PXA and 50% eGBs with 100% concordance between immunohistochemistry and sequencing. EGFR amplification was observed in 14% eGB's and 66% of 1° GB's. PDL1 and CTLA-4 expression was higher in eGB's (71.4% & 57.1%), A-PXA (66.6% &100%) and PXA (60% & 66.7%) as compared to 1° GB's (38.8% & 16.7%). T cell infiltration was also observed in majority of eGB's and PXA (90-100%) cases in contrast to 1°GB's (66%).

Conclusion

This is the first comprehensive analysis highlighting homogenous molecular profile and immune microenvironment of eGB and PXA, suggesting that they are closely related. Upregulation of PD-L1, CTLA4 and increased TIL's in these tumors suggests potential candidature for immunotherapy.

Introduction

Epithelioid glioblastoma is a rare provisional variant of IDH-wildtype GBs introduced in the 2016 WHO classification [1]. It is predominantly composed of solid aggregates or cohesive sheets of small to medium sized melanoma-like cell with variable "rhabdoid" features [2, 3]. Diagnosis is often challenging as there are no specific immunohistochemical (IHC) and molecular markers, with only few small series been reported till date. [3,4,5.6]. Most eGB's are recognized as de-novo tumors, however a few cases preceded by or concomitant with lower grade precursors have been reported [7, 8, 9]. Approximately 16.6–93 % of eGB's harbor *BRAF* V600E mutation, which is infrequent in other types of GBs [1, 5, 10].

eGB and PXA, especially A-PXA sometimes show overlapping cytological(discohesive epithelioid pattern and perivascular/intercellular lymphocyte infiltration) and molecular (*BRAF* V600E mutation) features

thus making the distinction between these subtypes occasionally difficult [2, 4, 7, 8]. There is a recent case report of eGB arising in a pre-existing PXA and studies documenting molecular overlap between the two entities [11, 2, 12,, 13].

Despite advances in therapy, prognosis for patients with GB remains dismal [14, 15]. Recently in field of neurooncology, there is a great interest to understand and evaluate the therapeutic potential of immunotherapies targeted towards activating and enhancing endogenous host immune responses including vaccines, adoptive T cell strategies and modulators of immune checkpoint regulators such as programmed death 1(PD-1), programmed death ligand 1(PDL-1) and cytotoxic T lymphocyte antigen 4(CTLA-4)[16, 17]. Immune-based treatments exert an indirect anti-tumor effect by generating potent, tumor-targeting immune responses and enhancing T cell functions [18]. Immune checkpoint inhibition has been shown to produce prolonged clinical remissions in subsets of patients with advanced solid organ malignancies like melanoma and small cell lung carcinoma [19]. Among brain tumors, many clinical trials using immune checkpoint blockers (ICB) are ongoing in patients with GB [20]. Owing to their rarity, there is no detailed study on status of PDL-1 and CTLA-4 expression in eGB's and PXA's.

This study was undertaken with the aim of analyzing the clinical, histopathologic and molecular profile of eGB's and PXAs to establish similarities and differences in the two groups. In addition PDL-1 expression, CTLA-4 expression and T-cell infiltration was assessed to identify genetic subgroups that could benefit from the targeted therapy and determine their prognostic significance.

Materials And Methods

Case selection

Histologically confirmed cases of eGB and PXA diagnosed over a 3-year period (2016–2018) were retrieved from the archives of four tertiary care hospitals.

Approval was obtained from institutional ethics committee for conducting experiments on human patient samples.
Cases having adequate tissue in paraffin blocks were identified. Fourteen eGB's and twenty-one PXAs (six A-PXA and 15 PXA) were included in the study. Eighteen 1° GB's were also taken to compare with there molecular and immune profile. Histopathological features were reviewed by two independent pathologists (VS, SM) according to the current WHO classification of CNS tumors. Patient demographics, tumor location and size, imaging findings, histopathological findings and clinical outcome were noted.

Immunohistochemistry

Immunostaining was performed on 5-microns thick formalin-fixed, paraffin-embedded tumor sections using an automated immunostainer (Benchmark XT, Ventana, Tucson, AZ, USA) and standard protocols including pretreatment using cell conditioning 1 buffer (Ventana) for 52 min and standard Ventana signal amplification. IHC was done using antibodies against Glial fibrillary acidic protein (GFAP, DAKO, Rabbit

polyclonal, 1:1000), CD34 (DAKO, Rabbit polyclonal, 1:100), epithelial membrane antigen (EMA, Cell Marque, mouse monoclonal, 1:100), vimentin (Santacruz, mouse monoclonal, 1:100), synaptophysin (Spring, Rabbit monoclonal, 1:100), Isocitrate dehydrogenase 1(IDH-1R32H, Dianova, mouse monoclonal, 1:50), alpha thalassemia/mental retardation syndrome X-linked (ATRX, Sigma-Aldrich, St. Louis, MO, USA dilution 1:400), P53 (Santa Cruz Biotechnology, Inc., CA, USA; dilution, 1:200), KI-67 ((DAKO, Glostrup, Denmark, Dilution 1:200)), mutation in 27th amino acid of Histone H3 (H3K27M, Millipore, Billercia, MA, USA, Dilution 1: 1000)), and INI-1 (Cell Marquee, mouse monoclonal, 1:100), PDL1 (SP263, Ventana, Tucson, AZ, USA, dilution 1:100), CTLA4 (Santa Cruz, dilution 1:75), cluster of differentiation 3(CD3, Dako, Glostrup, Denmark, dilution 1:100), cluster of differentiation 8 (CD8, Thermofisher Scientific, dilution 1:25). Diaminobenzidine was used as a chromogen. The presence and absence of markers including intensity, staining pattern and distribution was noted.

Staining for p53 was graded as 0 if no cells stained; 1 + if 0–10% stained; 2 + if 10–50% stained and 3 + if > 50% stained. Grade 2 + and above was considered positive [21]. For H3K27M expression, intense nuclear staining in more than 80% cells was taken as positive (21). For IDH, combined cytoplasmic and nuclear staining was interpreted as immunopositive and for ATRX expression; only nuclear staining was considered for evaluation. Cases with more than 10% positive tumor cells were scored positive. Endothelial cells, cortical neurons and infiltrating inflammatory cells were generally positive and served as internal positive controls. In cases with inhomogeneous immunoreaction, areas with the highest staining were scored. Tumours with > 1% of cells showing PDL-1 membrane staining of any intensity were considered positive. PDL-1 tumor proportion score (TPS) was calculated as a percentage of total tumor component showing focal/complete membranous staining of any intensity and was scored as weak (1–5%), moderate (> 5–25%), or strong (> 25%). Cytoplasmic, fibrillary and stromal PDL-1 staining was also observed occasionally but these cases were not considered positive, as the significance of non-membranous PDL-1 staining remains unclear. The CTLA-4 intensity of positive T cells were recorded as negative(0), weak(1–5%), moderate (6–25%) and strong (> 25%) based on percentage of lymphocytes showing positivity. For tumor infiltrating lymphocytes (TILs)- CD3 and CD8, the percentage of strongly positive cells over all nucleated cells was calculated using a hotspot approach. The whole tumor sections were scanned at a low power magnification (4x objective), and the areas of highest density of CD3 and CD 8 positive cells in direct contact with tumor cells at 400x visual field (40x objective × 10x ocular) were enumerated. Intra-vascular, perivascular and TILs in areas around zones of necrosis were excluded during counting.

Fluorescence In Situ Hybridization

Dual-probe fluorescence in situ hybridization (FISH) assay was performed on paraffin-embedded sections for assessment of EGFR amplification. Signals were scored in at least 200 non-overlapping, intact nuclei. Sections from non-neoplastic cortical tissue obtained from epilepsy surgery specimens were used as a control for each probe pair. Locus-specific probes paired with centromere probes for chromosomes 7 (CEP7, Vysis, Downers Grove, IL) was used for EGFR assay. EGFR amplification was considered when >

10% of tumor cells showed either an EGFR: CEP7 ratio of > 2 or innumerable tight clusters of signals of the locus probe [6].

Mutation analysis of BRAF V600E

DNA was extracted from 10-micron sections of formalin-fixed paraffin embedded (FFPE) tissue using the Recover all nucleic acid extraction kit using manufacturer's protocol (Invitrogen, Carlsbad, CA). DNA was quantitatively and qualitatively examined using Qubit (Invitrogen, Carlsbad, CA) and agarose gel. For all the cases, 50 ηg of total DNA was PCR amplified for detection of mutation in *BRAF* (codon 600). All PCR reactions were performed in a total of 20 micro litre reaction mixture using the Taq DNA polymerase (Invitrogen, Carlsbad, CA) with the following conditions: Denaturation at 95°C (10 min) followed by 42 cycles of denaturation at 95°C (30 s), annealing at 60°C (35 s) and elongation at 72°C (90 s). Bi-directional sequencing was performed using the Big Dye Terminator v3.1 Cycle Sequencing Kit (Applied Biosystems, Courtaboeuf, France) using the ABI 3500xL sequencer (Applied Biosystems, Foster City, CA) [6].

Statistical analysis

All statistical analyses were performed using IBM SPSS version 23 software (SPSS Inc., Chicago, IL). Associations among clinicopathological factors were tested using Fisher's exact test or non-parametric *t* test (Mann–Whitney test). Survival analysis was performed using the Kaplan–Meier method and the log-rank test. All statistical tests were 2-sided and $p < 0.05$ was considered statistically significant.

Results

Fourteen eGB's and twenty-one PXAs (including six A-PXA) were available for the study. There were 23 male and 12 female patients. Thirteen (37.2%) were pediatric and twenty-two (62.8%) were adult. Mean ages for PXA and eGB patients were 21.2 (range 11–42) and 30.9 (range 7–50) years, respectively. Most PXAs and eGB's occurred in the cerebral hemispheres while one each was seen in the cerebellum. The neuroradiological images showed similar nonspecific features that were peripheral smooth, well demarcated, contrast enhancing and localized superficial cerebral masses with perilesional edema. PXA in addition often had single and/or multiple cysts.

The median follow-up interval for all patients was 26 months (range 2–48months). 4 A-PXAs (66.67%) and 4 PXA (26.67%) recurred; the median interval to recurrence for the former was 14 months while for the latter was 28.5 months. Amongst the recurrence one case each of A-PXA (case 19) and PXA (case 21) progressed to eGB and one PXA progressed to A-PXA (Case 30). All the patients with eGB except two died of disease within 2 years of diagnosis, respectively. However, the two eGB patients still remaining alive at last follow-up (Cases 12 &13) with survival times already exceeding 2 years (26 and 32 months at last follow-up), suggests that long survival times are seen in this GB subset.

Histopathology and molecular features

Clinical, histopathological, immunohistochemical and molecular findings are summarized in Fig. 1a & b. PXA cases were characterized by spindled cells forming fascicles, scattered bizarre mono- and multinucleated cells with or without xanthomatous change, perivascular lymphocte cuffing, a dense pericellular reticulin network, and numerous eosinophilic granular bodies (EGB's)(Fig. 2a). A-PXAs in addition showed five or more mitosis, microvascular proliferation(MVP) and necrosis. However 4 of 6 cases of A-PXA (66.67%) also showed focal areas of epithelioid pattern of tumor cells, which lacked xanthomatous change, EGB's and reticulin fiber deposition (Fig. 2b). Two PXA/A-PXA (Case 19 and 21) cases, which transformed to eGB on follow-up, lost the pleomorphism and degenerative changes such as EGB's, reticulin fiber deposit and intracellular xanthomatous changes. The eGB's were composed almost exclusively of epithelioid cells, frequent mitoses and areas of necrosis (Fig. 2c) with three cases (21.4%) showing small foci (aproximately 5–10%) resembling astrocytic morphology. However none of the eGB's showed presence of EGB's or recticulin deposition.

Classical PXA were extensively positive for GFAP, synaptophysin, EMA and CD34 whereas these markers showed patchy and variable positivity in A-PXA and eGB's. The vimentin immunostain was diffusely positive in all the cases. The MIB-1 labeling index was high in eGB's (mean = 31.2%) and APXA (mean = 16.1%) as compared to classical PXA (mean = 4%). MIB1 labeling index was low in the PXA areas of A-PXA and high in the epithelioid areas. Similarly it was low in astrocytic areas noted in eGB's. All tumors had wildtype IDH1 (R132H) and retained ATRX and INI1 expression. None of the tumors expressed H3K27M mutant protein. P53 expression was also higher in eGB (8/14, 57%) and A-PXA (2/6, 33.33%) than PXA (2/15,13.33%) cases. *BRAF* V600E mutation was detected in 10 PXA's (66.67%), 2 APXAs (33.33%, both PXA and eGB components), and in 7 eGBs cases (50%). Interestingly, one A-PXA (Case 19) without and one PXA (Case 21) with *BRAF* V600E mutation acquired CDKN2A homozygous deletion at recurrence and transformed to eGB on follow up (Fig. 2d). None of the 1° GB's showed *BRAF* V600E mutation. There was 100% concordance between *BRAF* V600E mutation detection by IHC and Sanger sequencing)(Fig. 2e,f,i,j). Cases with positive *BRAF* mutation were associated with longer median progression free survival (PFS) of 27 months vs 16.5 months in those with absent mutation (P-value = 0.023), however overall survival (OS) analysis did not reach was statistical significance (P-value = 0.125) (Fig. 2g,h). None of the PXA or A-PXA cases showed EGFR amplification. However 14.2% eGBs showed EGFR amplification in contrast to 1° GB's which showed amplification in 66.66%, thus pointing towards the fact that eGBs are distinct from 1° GB's on molecular bases as well.

Immune profile

Immune profile findings are summarized in Fig. 3.

PD-L1 expression

PDL1 expression was more frequent in eGBs (71.4%,), A-PXA (66.6%) and PXA (60%) as compared to 1° GB (44.4%)(Fig. 4a). Though median percentage of PDL-1-expressing tumor cells was higher in eGB (3%, range: 0–90%), A-PXA (2%, range: 0–40%) and PXA, (2%, range: 0–60%) as compared to 1° GB (0%, range 0–90%)(Fig. 4b), more than 50% of cases in all the tumor subgroups showd weak to moderate PDL-1

TPS(Fig. 4c). However these differences did not meet statistical significance (eGB/PXA vs 1° GB P-value = 0.097 and 0.342)). Further we could not elucidate any association of PDL-1 expression with *BRAF* mutation (P value = 0.28), age (P value- 0.622), gender P value-0.26), PFS (P-value = 0.841) or OS (P-value = 0.33) (Fig. 4f-g).

CTLA4 expression

Maximum frequency of CTLA4 expression was observed in A-PXA (100%) followed by PXA (66.7%) and eGB (57.1%) while it was significantly low in 1°GB's (16.7%)(eGB/PXA vs 1°GB P-value = 0.001(Fig. 5a). Though majority of the positive cases under all subtypes showed only weak expression, it expression intensity was notably higher in eGB and PXA (eGB/PXA vs 1°GB P-value-=0.0008)(Fig. 5b-c), however we could not find any correlation with PDL-1 (P-value = 0.075) or overall survival (P-value = 0.1286).

Quantitative analysis of tumor-infiltrating lymphocytes

CD3 and CD8 expression was seen in 92.9%-100% cases of eGB, PXA and A-PXA, however only 66.7% and 55.6% cases of 1°GB's showed positivity for these markers (P-value = 0.001 each) (Fig. 5d). The tumor-infiltrating cytotoxic T lymphocytes (CTL) density among all subtypes ranged from 0 to up to 40 CTLs/ 100 tumor cells, and mean number of CD3 and C8 was significantly higher among eGB [20.3 (range 5–40, median 20) and 11.2 (range 0–40, median 8.5)], A-PXA [25.3 (range 7–40, median 25) and 12.5 (range 5–25, median 10)] and PXA [15.6 (range 2–40, median 15) and 10.6(range 2–25, median 10)] as compared to 1°GB [7.8 (range 0–30, median 4) and 3 (range 0–15, median 1)](P-value = 0.0004 and 0.0001) (Fig. 5e-f)). In addition we noted that the proportion of tumor cells expressing PDL-1 significantly correlated with increasing density of TIL's/100 tumor cells in all tumor subtypes (Spearman correlation co-efficient r = 0.29, p = 0.03)

Discussion

Recently studies have shown that sometimes PXAs particularly anaplastic PXAs show considerable clinical, radiological, histological and molecularly overlap with eGBs resulting in difficulties when attempting to segregate these entities [2, 3, 7]. Though eGB occurs in de novo fashion in the majority of cases, some cases arose from lower-grade gliomas as well [7, 8, 9, 11, 22]. The fact that most of these lower-grade lesions documented so far were PXA and that both tumors commonly exhibit *BRAF* V600E mutation re-enforce the possibility that eGB and PXA are related [2, 11, 23]. Two independent studies in addition revealed a striking similarity of genetic alterations (*BRAF* V600E, TERT promoter mutations and CDKN2A/B homozygous deletions) in anaplastic PXAs and eGBs [24, 25]. Further, eGBs have shown PXA or astrocytoma like areas with presence of *BRAF* mutation in both components [5, 8, 26], thus suggesting that *BRAF* mutation might possibly be an early event to both tumors and additional genetic alterations such as TERT-p, LSAMP or CDKN2A, is essential for progression of PXA to eGB. [5, 13, 27]. Supporting this hypothesis were our two cases of PXA and A-PXA that progressed to eGB after acquiring CDKN2A

homozygous deletion. Tanaka *et al* also recently reported a case of eGB developing within the tumor bed of a PXA, thirteen years after initial resection [11].

A recent study by Kurshonov *et* al documented considerable molecular and clinical heterogeneity within the eGBs by global DNA methylation and CNV analyses and established three distinct subsets: a PXA subset, with a high percentage of *BRAF* V600E mutations, but a relatively low percentage of TERT promoter mutations; an adult IDH-wild-type GB subset, with a relatively low percentage of *BRAF* V600E mutations, but a high percentage of TERT promoter mutations; and a pediatric RTK1 subset not harboring either mutation. They proposed that it is likely that the “epithelioid” GB phenotype represents a mere histologic pattern rather than a variant or separate entity [12].

In the current study PXA/A-PXA and e-GB exhibited some common findings on MRI: (i) contrast-enhanced solid and/or cystic; (ii) well circumscribed with no or little peritumoral edema; (iii) leptomeningeal involvement and dissemination. Histologically areas resembling PXA with focal lack of cytological uniformity along with spindled cells forming fascicles, few bizarre multinucleated cells, accompanied with infiltrating lymphocytes and perivascular lymphocytic cuffing were identified in three of fourteen (21.4%) eGB’s. However it was relatively inconspicuous in comparison to the adjacent, more abundant epithelioid rhabdoid looking tumor component as it constituted around 5–10% of the entire tumor raising the possibility that at least in few eGB’s, a precursor PXA component may be overgrown by the more malignant epithelioid component or was not sampled in the resection specimen. Mitotic figures, MVP and necrosis were found in both eGBs and A-PXA. Further, no reliable IHC or molecular differences were observed between the two glioma subtypes. In addition in our series A-PXA behaved clinically similar to eGB’s, with recurrences and death of a patient within 26 months of initial resection. All these findings suggest that eGB and PXA particularly A-PXA are either the same entity or highly related.

eGBs differs from conventional GB’s in that its course is often complicated by early recurrence, intratumoral hemorrhage and leptomeningeal spread and in addition it does not show EGFR amplification, IDH1 gene mutation or PTEN deletion, but instead, about 16.6–93% of these cases harbor *BRAF* V600E mutation [3, 8], a finding that remained true in our study as well.

In our study 100% concordance was found between Sanger sequencing and IHC results for *BRAF* V600E mutation, thus immunostaining could be used as a subsitute and cost-effective method for verification of the mutation. However any negative or low staining cases may be selected to undergo genetic analysis based on other clinical and histopathologic features. Other studies have also documented a high concordance between IHC and ARMs/Sanger sequencing with senstivity and specificity of IHC staining being 97–100% [28.29].

With the success of Immune checkpoint blockade (ICB) in various solid organ malignancies, the potential candidature of brain tumors for ICB is now being actively explored. Recent studies have reported PDL-1 and CTLA4 expression in GBs, which are targetable by prospective immunotherapies. Quantification of PDL-1 expression on tumor cells and CTLA-4 on T lymphocytes by IHC is widely being used as a predictive biomarker for ICB response [17, 30]. Adaptive upregulation of PDL-1 as an immune escape

mechanism is usually seen in tumors with increased CTL infiltrates [31]. A recent clinical trial reported lack of response to ICB in a small cohort of recurrent GBs despite PDL-1 expression and attributed the failure to the scarcity of intra-tumoral T-lymphocytes [32]. Hereby we used a simplistic approach of IHC for PDL-1, CTLA-4, CD3 and CD8 to identify whether eGB's and PXA are potential candidates for ICB.

In our small cohort the frequency and TPS of PDL-1 expression in PXA and eGB's was found to be higher than 1°GB though the difference could not meet statistical significance p-value = 0.097 and 0.342). The frequency of PDL-1 expression was 71.4% in eGB, 66.67% in APXA and 60% in PXA as compared to 1°GB (44.4%). Although overall positivity rate reported in adult gliomas is 44.72%, a wide range of PDL-1 expression (6.1 to 100%) has been noted across different studies [33]. Contrary to the studies on gliomas by Garber *et al* and Bergoff *et al* who documented high frequency of PDL-1 expression in only grade IV tumors, we observed its higher expression in PXA (grade II) and A-PXA (Grade III) cases [34, 35]. Although limited, the available studies present considerable differences in correlating PDL-1 expression with the patient outcome. In meta-analysis of 1052 patients, Xue *et al*. demonstrated high/positive PDL-1 expression to be associated with poor OS, which was also documented by Nduom *et a*l [36, 37]. However Berghoff *et al* and Heiland *et al* observed no association of PDL-1 with OS [35, 38]. In present study also we could not elucidate any association between PDL-1 positivity and OS or PFS in tumor subtypes. Further, in all tumor subtypes, there was no association of PDL-1 with any specific genetic alteration (Fig. 2).

Both frequency and intensity of CTLA-4 expression was found to be significantly higher in eGB and PXA cases as compared to 1°GB respectively (P-value = 0.001 and 0.0008). Though CTLA-4 is a well studied immune checkpoint protein, its expression in glioma and its effects on prognosis was yet not examined until recently Liu *et al* in his study documented that CTLA-4 have a positive correlation with PD-1 and TIL's and its higher expression are observed in higher grades of glioma and resulted in poor OS [39]. Though no association of CTLA-4 with overall survival was documented in our study (P-value = 0.1286), a variety of clinical trials targeting CTLA-4 have demonstrated promising benefits in patients with glioma therefore comprehensive analysis of CTLA-4 expression will still be required to identify its enrichment criteria in gliomas [40].

Frequency and density of TIL's expression was significantly higher in PXA (100% for both CD3 and CD8) and eGB (CD3-100%, CD8-92.9%) cases as compared to 1°GB (CD3-66.7%, CD8-55.6%) (P-value = 0.001 each, P-value = 0.0004 and 0.0001). Our findings were concordant with previous study by Berghoff *et al* and Kim *et al* who reported CD3 expression in 66.7 to 89.6% and CD8 expression in 44.4 to 77.6% GB's [35, 41]. Though there was statistically no significant difference between low and high-density groups of TIL with respect to overall survival in our study (p-value = 0.21), few studies have observed prolonged survival with increased TIL [41, 42]. However Hans documented that CD8 + TILs alone cannot effectively predict patient outcome in GB whereas high CD4 + TIL levels in combination with low CD8 + TIL levels were associated with unfavourable prognosis [43].

We acknowledge that the power of survival analyses in our series is limited by the sample size and the retrospective study design, and our results surely need confirmation in larger and prospectively collected cohorts. These observations together offer some circumstantial evidence that PXA and eGB's are more immunogenic thus reinforcing exploitation of PD-1/PDL-1 and CTLA-4 immune checkpoints for immune evasion.

Conclusion

This comprehensive analysis highlights homogenous molecular profile of eGBs and PXA, suggesting that they are closely related. In addition increased TIL densities and upregulation of PDL-1 and CTLA4 in these tumors suggests potential candidature for immunotherapy. Clinical trials with specific immune checkpoint inhibitors are warranted and it remains to be explored whether PDL-1/TIL expression patterns, patient's age or molecular alterations will correlate with response to such treatments.

Declarations

Acknowledgement: All staff of Neuropathology and Neurosurgery Department of AIIMS, New Delhi for support in accomplishment for this work.

Funding: JC Bose fellowship of Dr. Chitra Sarkar

Conflicts of interest: The authors have no conflict of interest to declare that are relevant to the content of this article

Availability of data and material: Yes

Code availability: Not applicable

Authors' contributions:

Dr. Swati Mahajan(SM) contributed to collecting data, designing, drafting of the manuscript and data interpretation of FISH and IHC.

Ms. Iman Dandapath, Ms Jyotsna Singh and Dr. Prerna Jha performed experiments (DNA isolation, Sanger sequencing) and reviewed their portion of work

Dr.Sujata Chaturvedi, Dr.Arvind Ahuja, Dr.Meenakshi Bhardwaj and Dr. Ravindra Saran provided cases, clinical data and follow up details of the patient.

Dr. Niveditha Manjunath and Dr. Ashish Suri provided clinical recordings and follow-up details of patients.

Dr. Ajay Garg contributed by providing radiological data

Dr. Vaishali Suri(VS), Dr. Mehar Chand Sharma and Dr. Chitra Sarkar aided in histopathological data analysis, interpretation and design of the work by giving valuable insights.

All authors finally approved the version to be published.

Ethics approval: Ethics approval was taken from AIIMS Ethics Institute.

Consent to participate: Yes

Consent for publication: Yes

References

1. Louis DN, Ohgaki H, Wiestler OD, Cavenee WK (2007) WHO Classification of Tumours of the Central Nervous System, 4th edn. IARC: Lyon.International Agency for Research on Cancer(IARC),2016;p58-p61

2. Alexandrescu S, Korshunov A, Lai SH et al (2016) Epithelioid glioblastomas and anaplastic epithelioid pleomorphic xanthoastrocytomas - same entity or first cousins? Brain Pathol 26:215-23. https://org/10.1111/bpa.12295.

3. Broniscer A, Tatevossian RG, Sabin ND, et al (2014) Clinical, radiological, histological and molecular characteristics of paediatric epithelioid glioblastoma. Neuropathol Appl Neurobiol 40:327-336. https://org/10.1111/nan.12093.

4. Kleinschmidt-DeMasters BK, Alassiri AH, Birks DK, Newell KL,Moore W, Lillehei KO (2010) Epithelioid versus rhabdoid glioblastomas are distinguished by monosomy 22 and immunohistochemical expression of INI-1 but not claudin 6. Am J Surg Pathol 34:341–354. https://doi.org/10.1097/PAS.0b013e3181ce107b.

5. Nobusawa S, Hirato J, Kurihara H, Ogawa A, Okura N, Nagaishi M et al (2014) Intratumoral heterogeneity of genomic imbalance in a case of epithelioid glioblastoma with BRAF V600E mutation. Brain Pathol 24:239–246. https://org/10.1111/bpa.12114.

6. Khanna G, Pathak P, Suri V et al (2010) Immunohistochemical and molecular genetic study on epithelioid glioblastoma: Series of seven cases with review of literature. PatholResPract 214:679-685. http://org/10.1016/j.prp.2018.03.019.

7. Kuroda J, Nobusawa S, Nakamura H et al (2016) A case of an epithelioid glioblastoma with the BRAF V600E mutation colocalized with BRAF intact low-grade diffuse astrocytoma. Neuropathology 36:181-186. https://org/10.1111/neup.12258.

8. Matsumura N, Nakajima N, Yamazaki T et al (2017) Concurrent TERT promoter and BRAFV600E mutation in epithelioid glioblastoma and concomitant low-grade astrocytoma. Neuropathology 3758-

63. https://doi.org/10.1111/neup.12318

9. Kanamori M, Suzuki H, Takei H, Sonoda Y, Uenohara H, Tominaga T (2016) Malignant transformation of diffuse astrocytoma to glioblastoma associated with newly developed BRAF V600E mutation. Brain Tumor Pathol 33: 50–56. https://org/10.1007/s10014-015-0231-7.

10. Robinson GW, Orr BA, Gajjar A (2014) Complete clinical regression of a BRAF V600E-mutant pediatric glioblastoma multiforme after BRAF inhibitor therapy. BMC Cancer 14:258. https://doi.org/10.1186/1471-2407-14-258

11. Tanaka S, Nakada M, Nobusawa S et al (2014) Epithelioid glioblastoma arising from pleomorphic xanthoastrocytoma with the BRAF V600E mutation. Brain Tumor Pathol 31: 172–176. https://doi.org/10.1007/s10014-014-0192-2

12. Korshunov A, Chavez L, Sharma T et al (2018) Epithelioid glioblastomas stratify into established diagnostic subsets upon integrated molecular analysis. Brain Pathol 28:656-662. https://doi.org/10.1111/bpa.12566

13. Furuta T, Miyoshi H, Komaki S et al (2018) Clinicopathological and genetic association between epithelioid glioblastoma and pleomorphic xanthoastrocytoma. Neuropathology 38:218-227. https://doi.org/10.1111/neup.12459

14. Stupp R, Mason WP, van den Bent MJ et al (2005) European Organisation for Research and Treatment of Cancer Brain Tumor and Radiotherapy Groups; National Cancer Institute of Canada Clinical Trials Group. Radiotherapy plus concomitant and adjuvant temozolomide for glioblastoma. N Engl J Med. 352:987-96. https://doi.org/10.1056/NEJMoa043330

15. Weller M, van den Bent M, Hopkins K et al (2014) European Association for Neuro-Oncology (EANO) Task Force on Malignant Glioma. EANO guideline for the diagnosis and treatment of anaplastic gliomas and glioblastoma. Lancet Oncol 15:e395-403. https://doi.org/10.1016/S1470-2045(14)70011-7

16. Ichikawa M, Chen L (2005) Role of B7-H1 and B7-H4 molecules in down-regulating effector phase of T-cell immunity: novel cancer escaping mechanisms. Front Biosci 10:2856-60. https://org/10.2741/1742.

17. Ohaegbulam KC, Assal A, Lazar-Molnar E, Yao Y, Zang X (2015) Human cancer immunotherapy with antibodies to the PD-1 and PD-L1 pathway. Trends Mol Med 21:24-33. https://org/10.1016/j.molmed.2014.10.009.

18. Reardon DA, Okada H (2015) Re-defining response and treatment effects for neuro-oncology immunotherapy clinical trials. J Neuroonco 123:339-46. https://org/10.1007/s11060-015-1748-7.

19. Topalian SL, Hodi FS, Brahmer JR, et al (2012) Safety, activity, and immune correlates of anti-PD-1 antibody in cancer. N Engl J Med 366:2443-54. https://org/10.1056/NEJMoa1200690.

20. Preusser M, Lim M, Hafler DA, Reardon DA, Sampson JH (2015) Prospects of immune checkpoint modulators in the treatment of glioblastoma. Nat Rev Neurol 11:504–514. https://org/10.1038/nrneurol.2015.139.

21. Jha P, Manjunath N, Singh J et al (2019) Analysis of PD-L1 expression and T cell infiltration in different molecular subgroups of diffuse midline gliomas. Neuropathology 39:413-424. https://doi.org/10.1111/neup.12594.

22. Suzuki Y, Takahashi-Fujigasaki J, Akasaki Y et al(2016) BRAF V600E-mutated diffuse glioma in an adult patient: A case report and review. Brain Tumor Pathol 33: 40–49. https://org/10.1007/s10014-015-0234-4.

23. Miyahara M, Nobusawa S, Inoue M, Okamoto K, Mochizuki M, Hara T (2016) Glioblastoma with Rhabdoid Features: Report of Two Young Adult Cases and Review of the Literature. World Neurosurg 86:515.e1–e9. https://org/10.1016/j.wneu.2015.10.065.

24. Phillips JJ, Gong H, Chen K et al (2019) The genetic landscape of anaplastic pleomorphic xanthoastrocytoma. Brain Pathol 29:85–96. https://doi.org/10.1111/bpa.12639.

25. Nakajima N, Nobusawa S, Nakata S et al(2018) BRAF V600E, TERT promoter mutations and CDKN2A/B homozygous deletions are frequent in epithelioid glioblastomas: a histological and molecular analysis focusing on intratumoral heterogeneity. Brain Pathol 28(5):663-673. https://dorg/10.1111/bpa.12572

26. Funata N, Nobusawa S, Yamada R, Shinoura N (2016) A case of osteoclast-like giant cell-rich epithelioid glioblastoma with BRAF V600Emutation. Brain Tumor Pathol 33: 57–62. https://org/10.1007/s10014-015-0239-z

27. Mistry M, Zhukova N, Merico D et al (2015) BRAF mutation and CDKN2A deletion define a clinically distinct subgroup of childhood secondary high-grade glioma. J Clin Oncol 33: 1015–1022. https://org/10.1200/JCO.2014.58.3922.

28. Long GV, Wilmott JS, Capper D et al (2013) Immunohistochemistry is highly sensitive and specific for the detection of V600E BRAF mutation in melanoma. Am J Surg Pathol 37:61-5. https://doi.org/10.1097/PAS.0b013e31826485c0.

29. Zhang X, Wang L, Wang J et al (2018) Immunohistochemistry is a feasible method to screen BRAF V600E mutation in colorectal and papillary thyroid carcinoma. Exp Mol Pathol 105:153-159. https://doi.org/10.1016/j.yexmp.2018.07.006.

30. Simonelli M, Persico P, Perrino M, et a; (2018) Checkpoint inhibitors as treatment for malignant gliomas: "A long way to the top". Cancer Treat Rev 69:121-131. https://doi.org/10.1016/j.ctrv.2018.06.016.

31. Spranger S, Spaapen RM, Zha Y, Williams J, Meng Y, Ha TT et al (2013) Up-regulation of PD-L1, IDO, and T (regs) in the melanoma tumor microenvironment is driven by CD8(+)T cells. Sci Transl Med 5:200ra116. https://org/10.1126/scitranslmed.3006504.

32. Groot JFD, Penas-Prado M, Mandel JJ, O'Brien BJ, Weathers SPS, Zhou S et al (2018) Window of opportunity clinical trial of a PD-1 inhibitor in patients with recurrent glioblastoma. J Clin Oncol 36:15_suppl, 2008-2008. https://doi.org/10.1200/JCO.2018.36.15_suppl.2008

33. Xue S, Hu M, Iyer V, Yu J (2017) Blocking the PD-1/PD-L1 pathway in glioma: a potential new treatment strategy. J Hematol Oncol 10:81. https://org/10.1186/s13045-017-0455-6.

34. Garber ST, Hashimoto Y, Weathers SP, et al (2016) Immune checkpoint blockade as a potential therapeutic target: surveying CNS malignancies. NeuroOncol 18:1357-66. https://org/10.1093/neuonc/now132.

35. Berghoff AS, Kiesel B, Widhalm G et al (2015) Programmed death ligand 1 expression and tumor-infiltrating lymphocytes in glioblastoma. Neuro Oncol 17:1064-75. https://doi.org/10.1093/neuonc/nou307.

36. Xue S, Song G, Yu J (2017) The prognostic significance of PD-L1 expression in patients with glioma: A meta-analysis. Sci Rep 7:4231. https://org/10.1038/s41598-017-04023-x.

37. Nduom EK, Wei J, Yaghi NK et al (2016) PD-L1 expression and prognostic impact in glioblastoma. Neuro Oncol 18:195-205. https://doi.org/10.1093/neuonc/nov172.

38. Heiland DH, Haaker G, Delev D, et l (2017). Comprehensive analysis of PD-L1 expression in glioblastoma multiforme. Oncotarget 8:42214-42225. https://doi:.org/10.18632/oncotarget.15031.

39. Liu F, Huang J, Liu X, Cheng Q, Luo C, Liu Z (2020). CTLA-4 correlates with immune and clinical characteristics of glioma. Cancer Cell Int 20:7. https://doi.org/10.1186/s12935-019-1085-6.

40. Hodges TR, Ott M, Xiu J et al (2017) Mutational burden, immune checkpoint expression, and mismatch repair in glioma: implications for immune checkpoint immunotherapy.NeuroOncol 19:1047-1057. https://doi.org/10.1093/neuonc/nox026.

41. Kim YH, Jung TY, Jung S, et al (2012) Tumour-infiltrating T-cell subpopulations in glioblastomas. Br J Neurosurg 26:21-7. https://org/10.3109/02688697.2011.584986.

42. Kmiecik J, Poli A, Brons NH, et al (2013) Elevated CD3+ and CD8+ tumor-infiltrating immune cells correlate with prolonged survival in glioblastoma patients despite integrated immunosuppressive

mechanisms in the tumor microenvironment and at the systemic level. J Neuroimmunol 264:71-83. https://org/10.1016/j.jneuroim.2013.08.013.

43. Han S, Zhang C, Li Q et al (2014) Tumour-infiltrating CD4(+) and CD8(+) lymphocytes as predictors of clinical outcome in glioma. Br J Cancer 110:2560-8. https://doi.org/10.1038/bjc.2014.162.

Figures

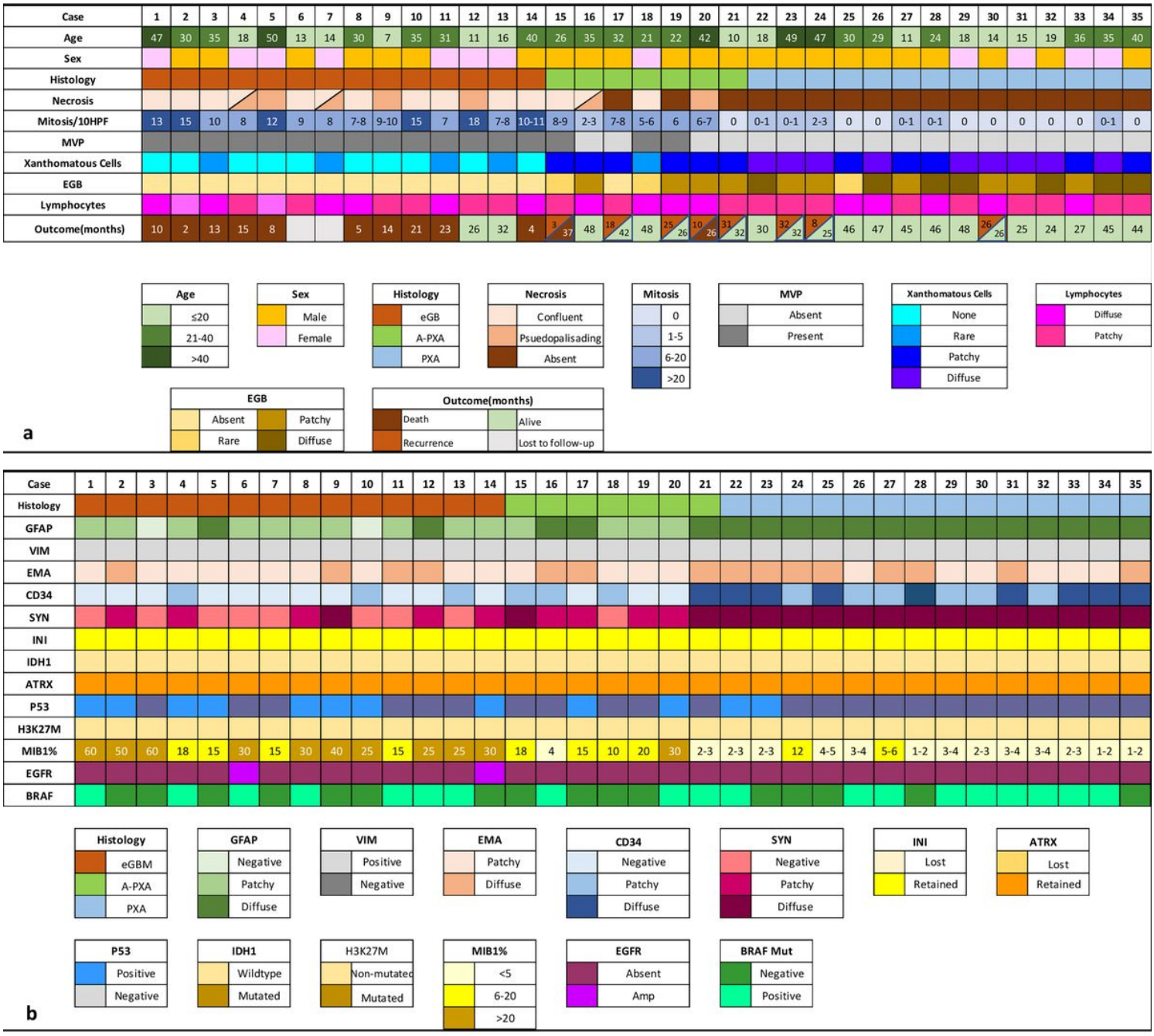

Figure 1

Clinicopathological (a) and immunohistochemical/molecular features (b) of tumors included in the study

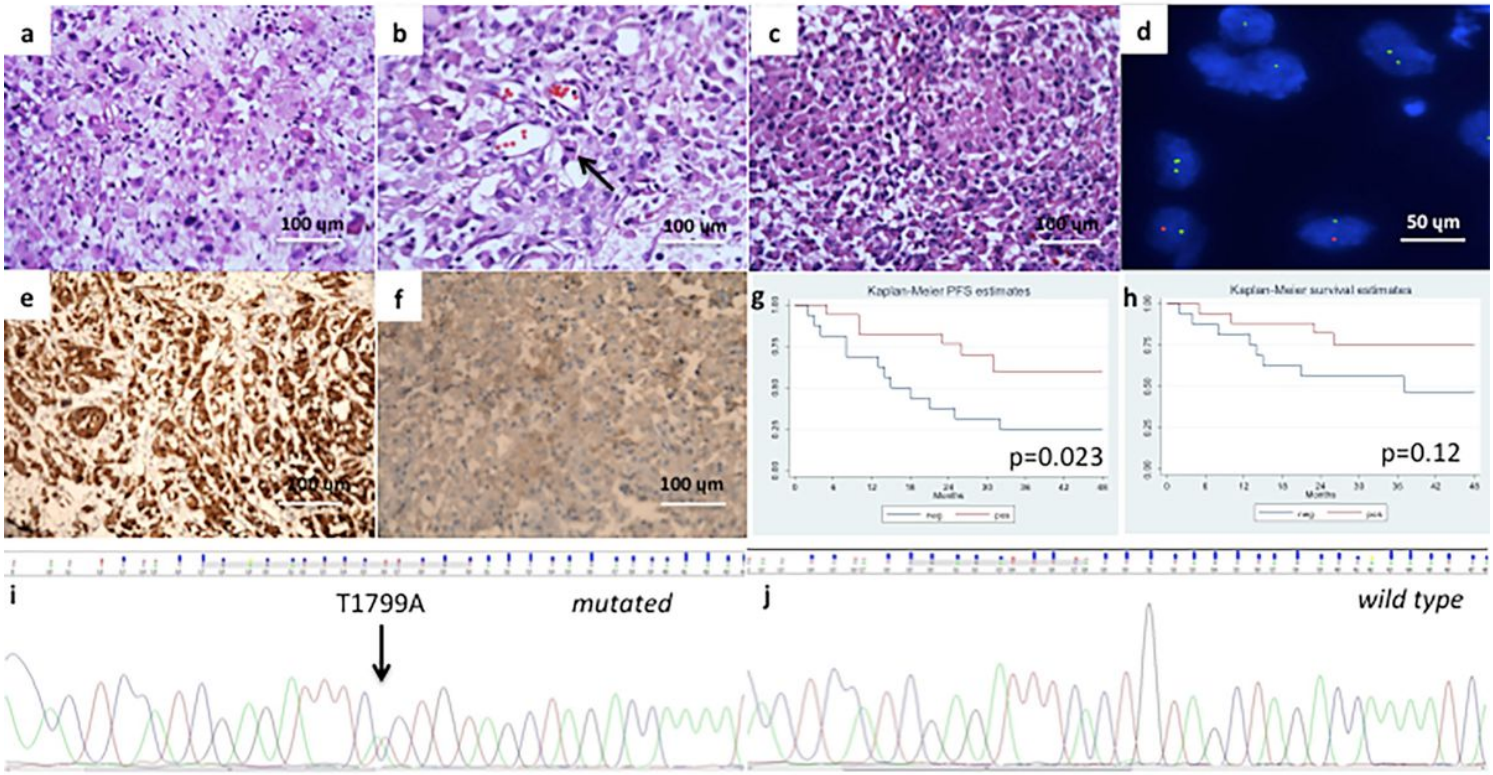

Figure 2

Hematoxylin and eosin (H&E) staining shows characteristic histological features of PXA (Case 26) composed of spindled to oval cells, showing prominent cellular pleomorphism along with mono-multinucleated giant cells and variable xanthomatous cells (a). H&E section of an epithelioid area in a case of A-PXA (case 19) demonstrating discohesive cells with abundant eosinophilic cytoplasm, eccentric nuclei, occasional nucleoli and distinct cellular borders (melanoma-like features) with high mitotic rate (arrow)(b). Microphotograph of an eGB (case 6), demonstrating sheets of epithelioid cells with the same features as described above(c) The tumor cells show CDKN2A/2B homozygous deletion on FISH assay (Case 19)(d). Examples of paired immunohistochemistry and sanger-sequencing results of a BRAF V600E mutated (e, i) and a wildtype case (f, j). Correlation of BRAF V600E mutation with progression-free survival (g) and overall Survival (h)

Case	1	2	3	4	5	6	7	8	9	10	11	12	13	14	15	16	17	18	19	20	21	22	23	24	25	26	27	28	29	30
Histology																														
PDL1%	80	2	0	2	5	10	0	2	0	50	70	3	0	90	2	2	0	40	0	4	10	0	0	6	0	0	60	2	40	0
CTLA4	0	3	0	0	0	8	3	4	0	0	4	3	2	2	3	2	2	5	3	3	3	0	1	2	0	3	2	0	2	0
CD3	25	40	40	5	20	5	20	30	5	5	40	10	10	20	15	20	7	40	30	40	10	10	5	15	20	40	15	30	15	25
CD8	10	20	40	3	15	2	10	20	3	0	30	5	2	7	5	5	5	25	20	15	10	8	5	10	20	10	8	15	7	25

Case	31	32	33	34	35	36	37	38	39	40	41	42	43	44	45	46	47	48	49	50	51	52	53
Histology																							
PDL1%	0	3	15	2	2	15	3	80	2	0	90	0	15	0	0	0	0	0	3	0	60	0	0
CTLA4	1	3	5	1	0	0	0	0	0	10	0	0	0	0	0	0	0	0	1	0	2	0	0
CD3	8	5	20	15	2	30	1	5	0	20	20	0	3	0	0	0	10	5	10	1	15	0	10
CD8	8	3	20	10	2	15	0	2	10	5	15	0	1	0	0	0	2	0	1	1	0	0	2

Histology	
	eGB
	A-PXA
	PXA
	GB

PDL1%	
0	absent
1-5	weak
6-25	moderate
>25	strong

CTLA4	
0	absent
1-5	weak
6-25	mod

CD3	
0	absent
1-5	low
>5	high

CD8	
0	absent
1-5	low
>5	high

Figure 3

Immune profile of the tumors included in the study

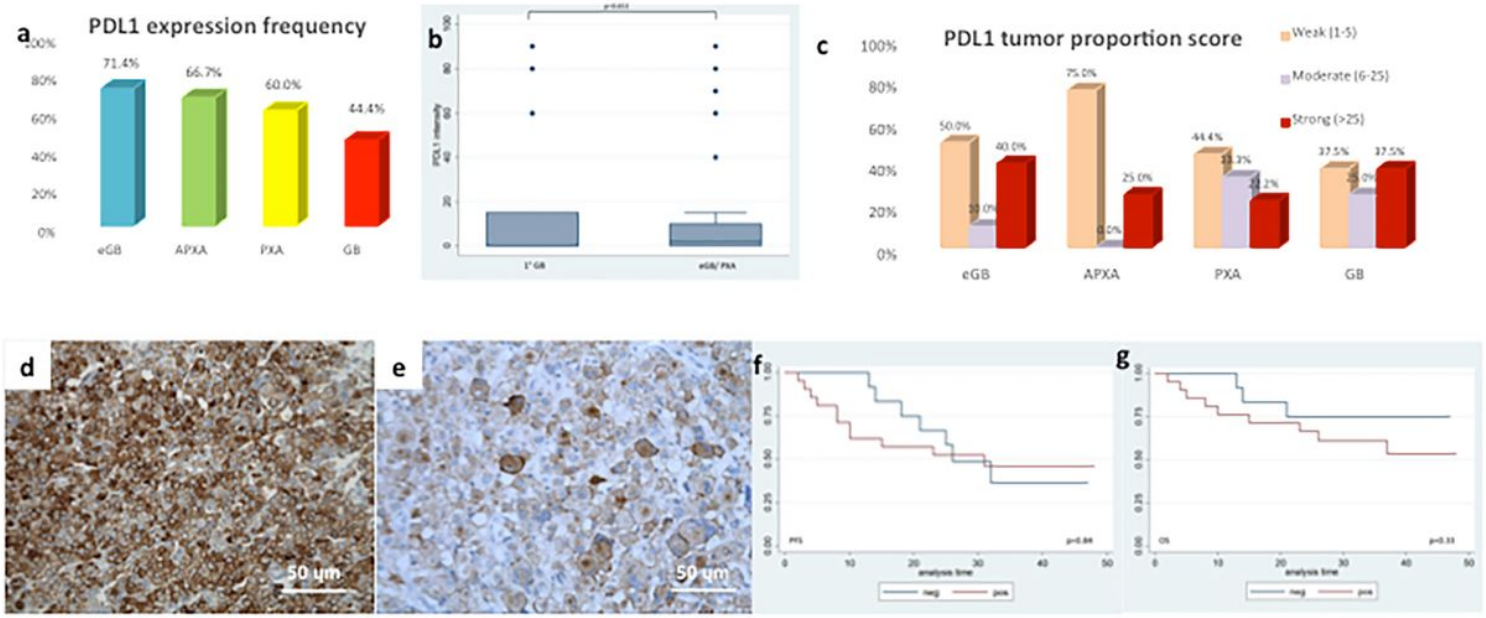

Figure 4

Quantitative analyses of PD-L1 expression frequency (a). Box and whisker plot for PDL-1 tumor proportion score in 1° GB vs eGB/PXA. Whiskers represent 5 and 95% confidence interval (b). PDL-1 tumor proportion score in tumor subgroups (c). Representative microphotographs of PDL-1 IHC showing membranous staining of tumor cells in a case of eGB (d) and PXA (e). Correlation of PDL-1 positivity with progression free survival (f) and overall survival (g)

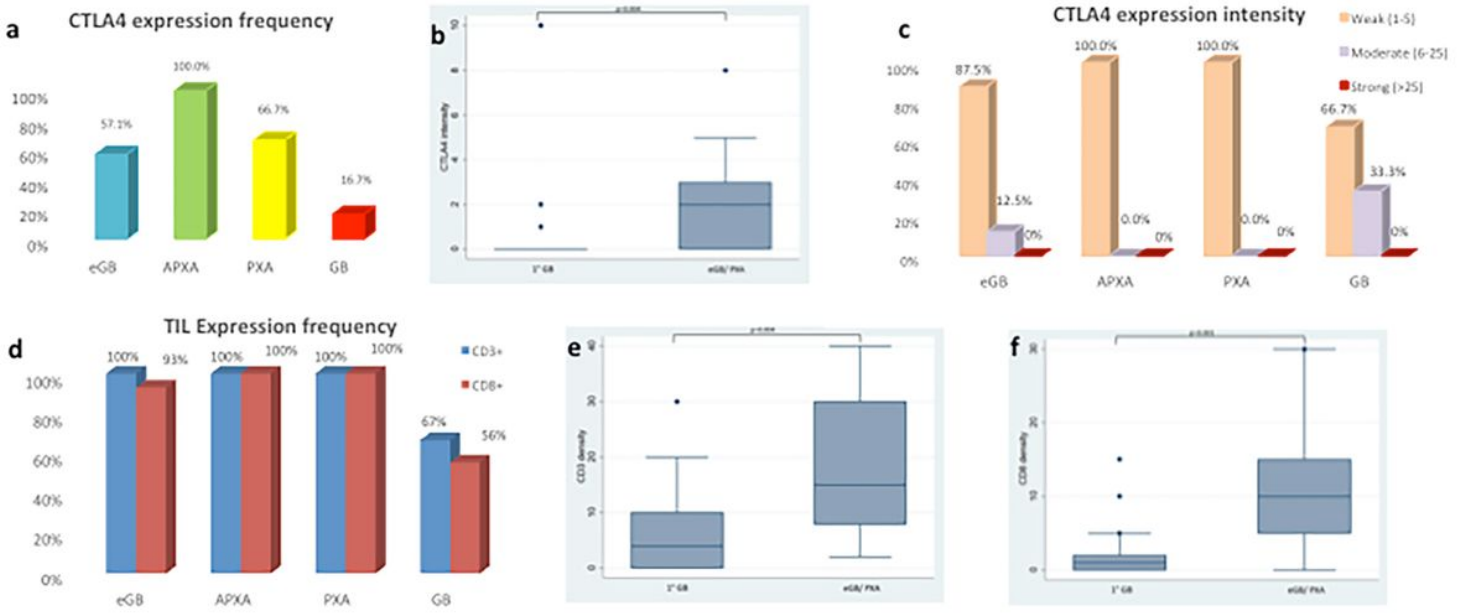

Figure 5

Quantitative analyses of CTLA-4 expression frequency (a Box and whisker plot for CTLA-4 intensity in 1° GB vs eGB/PXA. Whiskers represent 5 and 95% confidence interval (b). Staining intensity in tumor subgroups (c). Quantitative analyses of TIL's expression frequency (d) Box and whisker plot for CD3 and CD8 density in 1° GB vs eGB/PXA. Whiskers represent 5 and 95% confidence interval (e-f)